

Synthesis of Phytoalexins in Sorghum as a Site-Specific Response to Fungal Ingress

BETH A. SNYDER AND RALPH L. NICHOLSON*

Sorghum produces phytoalexins that are 3-deoxyanthocyanidin flavonoids. The compounds inhibit the growth of phytopathogenic fungi in vitro. The phytoalexins appear to be synthesized in subcellular inclusions within a host epidermal cell that is about to be penetrated by a fungus. This site-restricted synthesis suggests that the phytoalexin response occurs initially in the first cells that come under fungal attack and is not simply a response of cells that surround the original infection site.

PLANTS RESIST INFECTION BY PATHOGENS in various ways. One is the production of antimicrobial compounds, called phytoalexins, that kill the pathogen or restrict its intracellular development. Sorghum (*Sorghum bicolor* L.) is one of three monocotyledonous plants demonstrated to synthesize phytoalexins (1-3). Two phytoalexins, apigeninidin and luteolinidin, of the rare deoxyanthocyanidin class of flavonoids, are synthesized in juvenile sorghum as a response to attempted infection by the fungus *Colletotrichum graminicola* (Ces.) Wils. (2, 3). This pathogen causes the disease anthracnose, which is a problem worldwide, especially in developing nations of the semiarid tropics where sorghum is a staple food (4). Juvenile plants of both genetically resistant and susceptible cultivars synthesize the phytoalexins (2, 3) and resist the fungus. But as susceptible cultivars mature, they lose the ability to respond rapidly to fungal infection.

We have been investigating the resistance response of sorghum to identify early events that may serve as a basis for controlling anthracnose. One targeted event is phytoalexin synthesis, and an important question is where that synthesis occurs. We present evidence that phytoalexins in sorghum are synthesized in inclusions within the cell under attack. The inclusions move in the cell to the site of attempted penetration and release their contents into the cytoplasm, and additional phytoalexin synthesis occurs in surrounding cells.

In dicotyledonous plants the antimicrobial phytoalexins are synthesized in cells affected by the ingress of fungal pathogens (5). They are thought to be located in tissues surrounding the original infection site but not necessarily in cells initially penetrated (5, 6). It is difficult to determine the actual subcellular localization of phytoalexins because most are not visible. The time and

place of phytoalexin synthesis in any plant are critical to assigning temporal significance to the biosynthetic events that follow recognition and constitute the expression of resistance. Attempts to determine the location of synthesis include isolation of the compounds from tissues surrounding the infection site and their identification within an infection site (6). Such procedures, in conjunction with assays of enzymes involved in phytoalexin synthesis and analysis of expression of defense-related genes by in situ RNA hybridizations, reveal that phytoalexins should be synthesized in cells that are not yet infected (7) but do not indicate whether synthesis occurs in cells that are penetrated initially. Because the sorghum deoxyanthocyanidins are visible pigments that differ in color from other cell components of the plant (2), they present an opportunity to address the subcellular localization of phytoalexins.

To determine where the deoxyanthocyanidin phytoalexins are localized in sorghum, we inoculated the first leaf of 6-day-old seedlings (cv BR64) grown in growth chambers (28°C, 15-hour photoperiod) with spores (10⁶ spores per milliliter) of *C. graminicola*. Light microscopy of unfixed leaf pieces showed that mature appressoria, the fungal structures from which penetration occurs, had formed by 20 hours after inoculation. By 22 hours, colorless inclusions appeared in the cytoplasm of the targeted epidermal cell under attack (Fig. 1A). When the fungus attempted to penetrate at the junction of adjacent epidermal cells, inclusions accumulated in both cells. When first observed, inclusions were less than 1 µm in diameter; with time they enlarged (20 µm or larger) and coalesced. Inclusions moved toward the point of attachment of the fungal appressorium and by 24 hours became orange-red (Fig. 1B), a color that corresponds to the visible spectrum of the isolated phytoalexins (2, 3). With time the inclusions became even more intensely pigmented (Fig. 1C), and colorless inclusions could no longer be found. The pigmented inclusions lost their spherical shape and de-

posited their contents into the cytoplasm (Fig. 1D). Eventually the cell died. These events varied by no more than 2 or 3 hours between infection sites. Figure 1 is a chronological composite of the events observed to occur at several hundred different infection sites. After the pigments were released, they were observed to accumulate in the fungus. Pigment was progressively synthesized in cells immediately surrounding the original infection site. In leaves, the area of host response was shown to be restricted to approximately 2300 µm², equivalent to two to three cells per infection site (3).

Transmission electron microscopy (TEM)

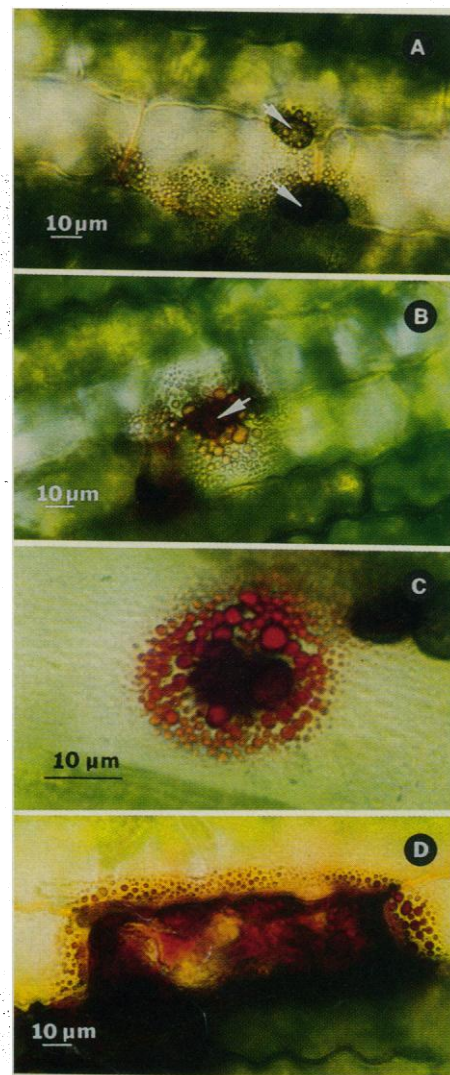


Fig. 1. (A) Surface view of a sorghum leaf inoculated 22 hours earlier with the fungus *C. graminicola*. Epidermal cells beneath fungal appressoria (arrows) contain colorless inclusions. (B) Inclusions move toward the point of attachment of the appressorium (arrow) and become pigmented. (C) The intensity of the inclusion pigmentation increases, and unpigmented inclusions are no longer evident by 30 hours after inoculation. (D) Inclusions release their contents into the cell 45 hours or more after inoculation. Surrounding cells contain pigmented inclusions.

Department of Botany and Plant Pathology, Purdue University, West Lafayette, IN 47907.

*To whom correspondence should be addressed.

of infected tissues revealed that after appressorium formation the cytoplasm of the underlying host cell became thickened. Host cytoplasm contained extensive endoplasmic reticulum (ER), ribosomes, and dictyosomes. These organelles were interspersed with spherical bodies containing an amorphous matrix (Fig. 2A). The time of appearance of the spherical bodies coincided with the time of appearance of the colorless inclusions observed by light microscopy. With time the spherical bodies enlarged, and this was followed by complete cell disruption and collapse. When cells collapsed, a densely staining amorphous material was observed on the inner surface of the host epidermal cell walls (Fig. 2B). Material with similar staining properties was frequently observed within appressoria after the collapse of the host cell (Fig. 2B). After epidermal cells collapsed, some mesophyll cells underlying the affected epidermal cell (or cells) showed abnormalities, including disruption of the chloroplast thylakoids and tonoplast (Fig. 2B). These mesophyll cells eventually col-

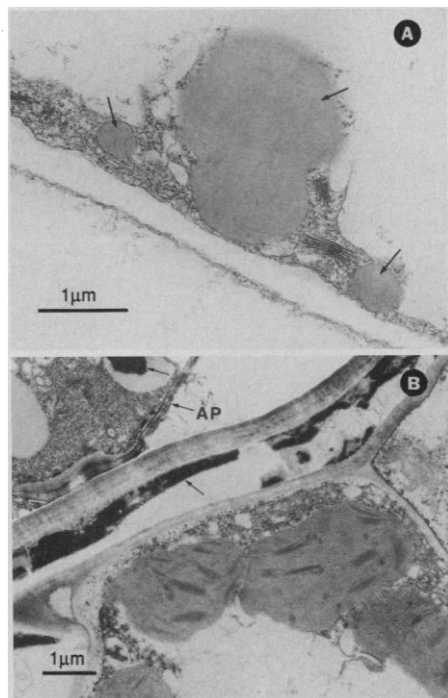
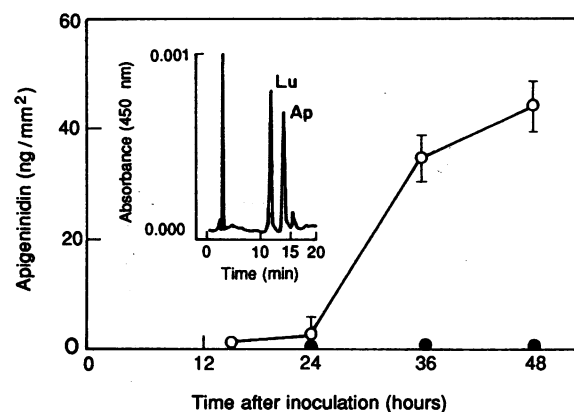


Fig. 2. Electron micrographs of leaves of *S. bicolor* inoculated with *C. graminicola*. (A) Inclusions (arrows) along epidermal cell walls underlying the site of attachment of a fungal appressorium 24 hours after inoculation. (B) Collapsed epidermal cells beneath a fungal appressorium (AP) 72 hours after inoculation. Densely staining, amorphous material is associated with the epidermal cell walls and within a fungal appressorium (arrows). Organelles in mesophyll cells show degradative changes. Tissue was fixed in 3% glutaraldehyde, 2.5% paraformaldehyde in 0.1 M sodium cacodylate buffer. Postfixation was in 2.0% osmium tetroxide. Tissue was dehydrated in ethanol and embedded in Spurr's resin.

Fig. 3. Accumulation in sorghum leaves of apigeninidin, a phytoalexin produced in response to fungal infection [(○) apigeninidin; (●) uninoculated control]. Inset shows the HPLC separation of apigeninidin (Ap) and luteolinidin (Lu) from tissue extracted 30 hours after inoculation with *C. graminicola*. Data represent the average of three replications of 50 infection sites per sample expressed as the mean \pm SEM.



lapsed. None of these events occurred in uninoculated tissues.

To determine when the phytoalexins began to accumulate relative to the time of the appearance of the pigmented inclusions, we removed individual infection sites, extracted the tissue, and separated the extracts by high-performance liquid chromatography (HPLC) (8). Apigeninidin and luteolinidin, the principal phytoalexins in sorghum, began to accumulate at 24 hours, the same time at which pigmented inclusions were first detected by light microscopy and spherical inclusions by TEM (Fig. 3).

The subcellular origin of flavonoid plant phenols is a subject of controversy with respect to both stress-induced synthesis of phytoalexins and synthesis of flavonoids in the apparent absence of stress. One line of evidence suggests that phenylpropanoids and flavonoids are synthesized in the ER, and substrates are channeled through multienzyme complexes (9). Other evidence suggests that anthocyanin flavonoids are synthesized in vesicles (anthocyanoplasts) ultimately located within the cell vacuole (10). The hypothesis that the vacuole is the general site of anthocyanin synthesis was challenged by the demonstration that anthocyanin methyltransferase, the final enzyme in the methylation of the anthocyanins of petunia, is cytosolic and not vacuolar (11). The accumulation and apparent synthesis of the sorghum phytoalexins in discrete cytoplasmic inclusions do not support the concept that synthesis occurs within a central vacuole. We presume that the inclusions are ER-Golgi apparatus derivatives but have not successfully resolved a characteristic unit membrane surrounding these structures by TEM.

Synthesis of phytoalexins in inclusions is supported by our observations that cytoplasmic inclusions first accumulate as clear spherical bodies and then become highly pigmented as they near the site of fungal ingress. The pigmented inclusions in sorghum resemble anthocyanoplasts, because

inclusions fuse, but differ from anthocyanoplasts, because they are cytoplasmic rather than vacuolar. Thus, the results of the present investigation are consistent with the hypothesis that phenols of the phenylpropanoid and flavonoid classes are synthesized within the cytoplasm (9, 11).

We have demonstrated that sorghum responds to infection by producing intensely pigmented, spherical bodies within the epidermal cells immediately under fungal attack. Only late in the infection process do cells surrounding the first infected cells respond by the production of similar structures. Because the accumulation of the red phytoalexin pigments corresponds to the appearance of the spherical, red bodies within infected cells, this research suggests that these bodies are the site of synthesis or accumulation of the sorghum phytoalexins.

REFERENCES AND NOTES

1. D. W. Cartwright and P. Langcake, *Physiol. Plant Pathol.* **17**, 259 (1980); ———, R. J. Pryce, D. P. Leworthy, J. P. Ride, *Phytochemistry* **20**, 535 (1981); S. Mayama, T. Tani, Y. Matsuura, T. Ueno, H. Fukami, *Physiol. Plant Pathol.* **19**, 217 (1980).
2. R. L. Nicholson, S. S. Kollipara, J. R. Vincent, P. C. Lyons, G. Cadena-Gomez, *Proc. Natl. Acad. Sci. U.S.A.* **84**, 5520 (1986).
3. R. L. Nicholson, F. F. Jamil, B. A. Snyder, W. L. Luc, J. Hipskind, *Physiol. Mol. Plant Pathol.* **33**, 271 (1988).
4. M. A. Pastor-Corrales and R. A. Frederiksen, in *Sorghum Diseases: A World Review* (International Crops Research Institute for the Semi-arid Tropics, Patancheru, India, 1980), pp. 289–299.
5. L. J. Halverson and G. Stacey, *Microbiol. Rev.* **50**, 193 (1986); J. Ebel, *Annu. Rev. Phytopathol.* **24**, 235 (1986); R. A. Dixon, P. M. Dey, C. J. Lamb, in *Advances in Enzymology*, A. Meister, Ed. (Wiley, New York, 1983), vol. 55, pp. 1–136.
6. W. Jahnen and K. Hahlbrock, *Planta* **173**, 197 (1988); J. E. Rahe, *Can. J. Bot.* **51**, 2423 (1973); J. W. Mansfield, J. A. Hargreaves, F. C. Boyle, *Nature* **252**, 316 (1974); S. Mayama and T. Tani, *Physiol. Plant Pathol.* **21**, 141 (1982); P. Moesta, U. Seydel, B. Lindner, H. Grisebach, *Z. Naturforsch. Teil C* **37**, 748 (1982).
7. J. N. Bell, T. B. Ryder, V. P. M. Wingate, J. A. Bailey, C. J. Lamb, *Mol. Cell. Biol.* **6**, 1615 (1986); E. Schmelzer, S. Kruger-Lebus, K. Hahlbrock, *Plant Cell* **1**, 993 (1989).
8. Individual infection sites were identified under the microscope and removed with a stainless steel borer (internal diameter, 0.67 mm). Three replicates of 50

disks each were collected at each time interval. The tissue was placed in absolute methanol for 18 hours. The methanol extract was removed, the tissue was washed with methanol, and the methanol fractions were combined. The final extract was dried under nitrogen and adjusted to 100 μ l with absolute methanol. Samples (50 μ l) were separated by HPLC on a C-18 reverse-phase column as described in (2).

9. H. A. Stafford, in *The Biochemistry of Plants*, E. E.

Conn, Ed. (Academic Press, New York, 1981), vol. 7, pp. 118–137; G. Hrazdina and G. J. Wagner, *Arch. Biochem. Biophys.* **237**, 88 (1985).

10. R. C. Pecket and C. J. Small, *Phytochemistry* **19**, 2571 (1980); C. J. Small and R. C. Pecket, *Planta* **154**, 97 (1982); M. Nozue and H. Yasuda, *Plant Cell Rep.* **4**, 252 (1985).

11. L. M. V. Jonsson, W. E. Donker-Koopman, P. Uitslager, A. W. Schram, *Plant Physiol.* **72**, 287

(1983).

12. Journal article 12356 of the Purdue University Agricultural Experiment Station (AES). Use of the AES Electron Microscopy Center is acknowledged. Supported in part by NSF grant DCB 89-05121 and the Indiana Corporation for Science and Technology.

19 January 1990; accepted 18 April 1990

Human CD4 Binds Immunoglobulins

PETAR LENERT, DANIEL KROON, HANS SPIEGELBERG, EDWARD S. GOLUB, MAURIZIO ZANETTI*

T cell glycoprotein CD4 binds to class II major histocompatibility molecules and to the human immunodeficiency virus (HIV) envelope protein gp120. Recombinant CD4 (rCD4) bound to polyclonal immunoglobulin (Ig) and 39 of 50 (78%) human myeloma proteins. This binding depended on the Fab and not the Fc portion of Ig and was independent of the light chain. Soluble rCD4, HIV gp120, and sulfated dextrans inhibited the CD4-Ig interaction. With the use of a panel of synthetic peptides, the region critical for binding to Ig was localized to amino acids 21 to 38 of the first extracellular domain of CD4. CD4-bound antibody (Ab) complexed with antigen approximately 100 times better than Ab alone. This activity may contribute to the Ab-mediated enhancement of cellular HIV interaction that appears to depend on a trimolecular complex of HIV, antibodies to gp120, and CD4.

THE GLYCOPROTEIN CD4 PARTICIPATES in adhesion of T lymphocytes to target cells (1), thymic development (2), and transmission of intracellular signals during T cell activation (3). CD4 is also the high-affinity receptor for HIV gp120 (4), an activity of amino acids 42 to 55 of the NH₂-terminal domain (5). This domain has an Ig-like fold, and residues 40 to 55 correspond to the second complementarity-determining region of human Ig κ light (L) chain (5).

In preliminary experiments, we observed that serum Ig from normal subjects bound soluble recombinant CD4 (rCD4) and CD4 solubilized from the CD4⁺ CEM cell line in enzyme-linked immunosorbent assay (ELISA) and radioimmunoassay (RIA). We therefore tested 50 human myeloma proteins of unknown antigen reactivity representing each class and subclass (Table 1). Thirty-nine of 50 (78%) myeloma proteins devoid of rheumatoid factor activity bound CD4 regardless of their heavy (H) or L chain isotype. The binding values varied among myeloma proteins of the same class,

subclass, and L chain type. Although all classes bound, none of the six myeloma proteins in the IgG4 subclass tested were positive, even at relatively high concentration (200 μ g/ml). Myeloma proteins representative of each Ig class were labeled with ¹²⁵I, and they displayed a single band of 46 to 50 kD in a protein immunoblot of soluble rCD4 (Fig. 1A). This was the same size as the band identified by Leu3a, a murine monoclonal antibody (MAb) to CD4. Whereas ¹²⁵I-labeled Ig binding was unaffected by electrophoresis of CD4 under reducing conditions, MAb Leu3a binding decreased after reduction. This suggests that the Ig binding site, unlike the Leu3a epitope (6), is less affected by the intactness of the three-dimensional conformation of the molecule. However, because it is generally accepted that partial renaturation takes place after blotting, the extent to which the tertiary structure of CD4 still influences Ig binding cannot be assessed with precision. Human Ig also bound CD4⁺ T cells. In flow cytometry, CEM cells were stained by polyclonal Ig with a unimodal peak, yielding a reproducible and consistent ($\sim 5 \times$) shift in the mean fluorescence intensity above that of control cells (Fig. 1B). By comparison, MAb Leu3a gave a mean fluorescence intensity ten times as great.

The relation of the Ig and gp120 binding sites of CD4 was analyzed in three ways. Soluble recombinant gp120 inhibited (50% inhibition at $< 1 \mu$ g of gp120 per milliliter) the binding of a ¹²⁵I-labeled human myelo-

ma protein to rCD4 in solid-phase RIA (Fig. 2A). Dextran sulfate, which blocks the binding of HIV to CD4⁺ cells and prevents infection in vitro (7), inhibited the CD4-Ig interaction (50% inhibition at $< 0.5 \mu$ g of dextran per milliliter), an effect apparently on CD4 because incubation with dextran sulfate followed by washing was equally

Table 1. Human myeloma proteins of different isotype bind rCD4. Binding of human myeloma proteins to soluble rCD4 in ELISA. Fifty purified human myeloma proteins representing all Ig classes and subclasses were tested. Polyvinyl chloride microtiter plates (Dynatech) were coated with soluble rCD4 (Receptin, Biogen) (3 μ g/ml) in 0.9% NaCl by incubating at 4°C overnight. Human myeloma proteins diluted (40 μ g/ml) in phosphate-buffered saline (PBS) containing 1% bovine serum albumin (BSA) and 0.5% Tween 20 (PBSA), were incubated for 3 hours at room temperature. Bound antibodies were revealed with a goat antibody to human Ig (H chain specific) conjugated to horseradish peroxidase (HRP) (Sigma) in PBSA containing 15% newborn calf serum. Detection of IgE and IgD required an intermediate incubation with goat antibodies to IgE or IgD, respectively, followed by HRP-conjugated swine antibody to goat Ig (Tago). Values represent the mean absorbance (A_{492}), which shows binding of myeloma proteins grouped by H chain isotype. SEM, $< 15\%$. The 40 μ g/ml concentration was chosen on the basis of pilot experiments in which the saturation points were determined with myeloma proteins of different classes. Saturation of binding was obtained at 40 μ g/ml for IgG, IgM, IgD, and IgE, and at 80 μ g/ml for IgA. By comparison, MAb Leu3a (Becton-Dickinson) specific for CD4 reached plateau at $\sim 4 \mu$ g/ml. A_{492} of the second antibody alone (1:1500) was less than 0.050. Values of A_{492} less than 0.2 were considered positive. By comparison, the binding value (A_{492}) of polyclonal human Ig human γ -globulins fraction II, Pentex, Miles) (40 μ g/ml) was 1.5 (see Table 2). Binding to a recombinant MAb (IgG2b, κ) (23) and to BSA (molecular weight 65,000) are specificity controls.

Myeloma protein	No. positive	Absorbance (A_{492})		
		rCD4	rIg	BSA
IgG1	4/6	0.61	0.13	0.14
IgG2	5/6	0.48	0.09	0.1
IgG3	6/6	0.58	0.15	0.15
IgG4	0/6	0.18	0.16	0.14
IgM	6/6	0.81	0.12	0.13
IgA1	3/5	0.36	0.11	0.12
IgA2	3/3	0.38	0.11	0.09
IgD	7/7	0.85	0.11	0.19
IgE	5/5	1.10	0.10	0.13

P. Lenart and M. Zanetti, Division of Dermatology, Department of Medicine, University of California, San Diego, San Diego, CA 92103.

D. Kroon, The R. W. Johnson Pharmaceutical Research Institute, Raritan, NJ 08869-0602.

H. Spiegelberg, Department of Immunology, Research Institute of Scripps Clinic, La Jolla, CA 92037.

E. S. Golub, Johnson & Johnson Laboratories, Research Institute of Scripps Clinic, La Jolla, CA 92037.

*To whom correspondence should be addressed.